# Small molecule-facilitated anion transporters in cells for a novel cystic fibrosis therapeutic approach

**Michele Fiore[1], Claudia Cossu[1], Valeria Capurro[2], Cristiana Picco[1], Alessandra Ludovico[1], Marcin Mielczarek[3], Israel Carreira-Barral[3], Emanuela Caci[2], Debora Baroni[1], Roberto Quesada[3], Oscar Moran[1*]**

[1] Istituto di Biofisica, CNR, Genova, Italy;

[2] U.O.C. Genetica Medica, Istituto Giannina Gaslini, Genova, Italy;

[3] Departamento de Química, Facultad de Ciencias, Universidad de Burgos, Burgos, Spain

*Corresponding author:

Oscar Moran
Istituto di Biofisica, CNR. Via De Marini, 6. 16149 Genova, Italy
Email address: oscar.moran@cnr.it.
Tel +39 0106475558

**Keywords**: cystic fibrosis, ionophore, ion transport, prodigiosines, tambjamines

**Running tittle:** Anionophores as a cystic fibrosis substitutive therapy

**Bullet point summary**

*What is already known:*

• The anion channel CFTR is defective in cystic fibrosis

*What this study adds:*

• Anionophores are small molecules capable to efficiently transport halides and bicarbonate across cell membranes.

• Anionophores do not interfere with the function and pharmacology of CFTR.

*Clinical significance:*

• Anionophores could be used as substitution therapy in cystic fibrosis.

**Abstract**

**Background and Purpose**

Cystic fibrosis (CF) is a lethal autosomal recessive genetic disease that originates from the defective function of the CFTR protein, a cAMP-dependent anion channel involved in fluid transport across epithelium. Due to their capability to replace the ion transport independently from the genetic mutation that affects the CFTR, small synthetic transmembrane anion transporters, named anionophores, are candidates as new potential CF therapeutics.

**Experimental Approach**

With the aim of evaluating their impact on cell physiology, we have analysed the transport properties of five compounds, three prodigiosines and two tambjamines.

**Key Results**

All studied compounds are capable of transporting halides and bicarbonate across the cell membrane, with a higher transport capacity at acidic pH. Interestingly, the presence of these anionophores do not interfere with the activation of CFTR, and do not modify the action of the lumacaftor and ivacaftor, a CFTR-corrector and -potentiator, respectively.

**Conclusion and Implications**

Their ability to transport chloride and bicarbonate when applied at low concentration take shape as a promising starting point for the development of novel CF-therapy drug candidates.

**Abbreviations**

BCECF: 2',7'-bis(2-carboxyethyl)-5-(and-6)carboxyfluorescein
CF: Cystic Fibrosis
CFTR: Cystic fibrosis tranmembrane conductance regulator
DIDS: 4,4'-diisiothiocanostilbene-2,2'-disulfonate
LUV: large unilamellar vesicles
NMDG: N-methyl-D-glucamine
OBX: obatoclax
$pH_i$: intracellular pH
POPC: 1-palmitoyl-2-oleoyl-sn-glycero-3- phosphocholine
PRG: prodigiosine
QR: fluorescence decay
YFP: yellow fluorescence protein

## Introduction

Cystic fibrosis (CF) is the most common autosomal recessive lethal genetic disease in the Caucasian population (Bobadilla et al., 2002; Strausbaugh and Davis, 2007). The major cause of CF morbidity and mortality is lung disease, which is characterised by infection, inflammation, and airway damage that leads to respiratory failure. More than 2000 mutations in CFTR, classified in six classes according to the effect of the mutation, lead to anion transport defects in epithelium by various mechanisms (failure to synthesise the protein, processing flaws, gating or conductance defects, reduced expression) (Castellani and Assael, 2017). The F508del mutation of the CFTR protein underlies most CF cases, causing a defective trafficking to the plasma membrane (class II mutation) and reduced activity of the channel preventing CFTR from undertaking its normal function (class III mutation). Efforts have been made to restore CFTR function by gene therapy or by using small organic compounds to ameliorate the disease (Galietta, 2013; Hudock and Clancy, 2017; Zegarra-Moran and Galietta, 2017). To address the reduced activity defect of G551D (class III mutations), and of other less frequent mutations the potentiator Ivacaftor, which improves chloride transport and lung function of patients, has been introduced (Ramsey et al., 2011). However, attempts to enhance chloride transport by using drugs that increase delivery of functional F508del-CFTR to the cell surface have been less successful. Lumacaftor, a CFTR corrector, has been found to increase the cell surface density of functional F508del-CFTR *in vitro* (Van Goor et al., 2011; Ren et al., 2013; Zegarra-Moran and Galietta, 2017), but has a very modest beneficial effects in patients (Clancy et al., 2012; Boyle et al., 2014; Wainwright et al., 2015; De Boeck and Davies, 2017). CF patients treated with a new corrector, VX-659, in combination with Lumacaftor and Ivacaftor, have shown a promising moderate amelioration (Davies et al., 2018)

An alternative strategy could be the use of molecules capable of transporting anions across lipid bilayers, named anionophores, to substitute the disfunctional transport in CF. In this regard, although several studies have been published recently, functional analyses of this type of molecules in cells are still very limited (Davis et al., 2010; Hernando et al., 2014a; Valkenier et al., 2014; Li et al., 2016; Wu et al., 2016; Li et al., 2017; Cossu et al., 2018; Dias et al., 2018). The idea of using anionophores to replace the defective CFTR protein has the advantage of becoming a general therapy for CF, that would be independent of the specific mutation. With this perspective, we have synthetised and characterised the transport properties of five anionophores. We have studied the natural product prodigiosine (Rapoport and Holden, 1962), the synthetic derivative obatoclax (Díaz de Greñu et al., 2011), the triazole derivative of prodigiosin, EH130 (Hernando et al., 2018), and two synthetic analogues of the marine alkaloids named tambjamines: RQ363 (Hernando et al., 2014b), and MM3. The last three compounds, EH130, RQ363 and MM3, are interesting because they retain a significant anion transport capacity, but have reduced cytotoxicity. Herein we show that these anionophores are capable of transporting relevant anions physiologically, such as chloride and bicarbonate, in mammalian cells, without a significant interference with the CFTR transport and pharmacology, either native or treated with drugs.

## Methods

### Synthesis of the anionophores

Anionophores prodigiosine (Rapoport and Holden, 1962), obatoclax (Díaz de Greñu et al., 2011), EH130 (Hernando et al., 2018) and RQ3634 (Hernando et al., 2014b) were synthesized as previosuly reported (see Figure 1A). MM3 was prepared by reaction of 3-ethyl-4-methyl-1H,1'H-[2,2'-bipyrrole]-5-carbaldehyde (250.9 mg, 1.24 mmol) with glacial acetic acid (50 µL) and cyclohexylamine (275 µL, 2.40 mmol, 1.94 equiv.) in chloroform (10 mL). The reaction mixture was stirred at 60 °C for 6 h. Upon cooling to room temperature the chloroform was evaporated under reduced pressure and the residue was re-dissolved in dichloromethane (30 mL). The solution of the crude compound MM3 was washed with 1 M aqueous HCl solution (3 × 20 mL), dried over anhydrous $Na_2SO_4$, filtered and evaporated to dryness under reduced pressure. The residue was re-crystallised from a mixture of dichloromethane and n-hexane to give compound MM3 as dark yellow needles (Yield: 264.2 mg, 67%). All compounds were fully characterised by mass spectrometry and NMR. Detailed characterization is provided in the Supplementary data. Purities of compounds were estimated by

$^{1}$H NMR to be greater than 96% for all tested compounds. Except when indicated, all chemicals were purchased from Sigma-Aldrich. The chemical structure of the studied compounds are shown in Figure 1A.

**Chloride efflux in phospholipid large unilamelar vesicles**

The activity of the transmembrane carriers was assayed in model 1-palmitoyl-2-oleoyl-sn-glycero-3- phosphocholine (POPC) large unilamellar vesicles (LUVs) with average diameters of 200 nm as described elsewhere (Soto-Cerrato et al., 2015; Cossu et al., 2018; Hernando et al., 2018). LUVs were prepared by extrusion across polycarbonate membranes (LiposoFast Basic extruder; Avestin, Inc.). The LUV were prepared in a high chloride solution (489 mM NaCl and 5 mM phosphate buffer, pH 7.2), and dialyzed against a nitrate solution (489 mM $NaNO_3$ and 5 mM phosphate buffer, pH 7.2), to remove the unencapsulated chloride. Final concentration of POPC in the experiments was 0.5 mM. The chloride efflux from chloride-loaded LUV was monitored recording the time course of the external chloride concentration using ion selective electrodes (Vernier, Beaverton, Oregon, USA or Hach Chloride Ion Selective Electrode, Loveland, Colorado, USA) Both chloride sensitive electrodes used have a measuring range of 1 mg/L to 35 g/L and a lineal response (voltage vs log concentration) of 55 ± 4 mV / decade at 20 ± 5 °C. Release of all encapsulated chloride by addition of detergent allows the normalization of the data. The anionophore activity was expressed as the normalised concentration realeased after 300 seconds. The relative potency of the anionophore transport was estimated as the concentration to induce 50% of the maximum chloride release in time interval.

**Cell viability and apoptosis**

Cell toxicity of anionophores was evaluated in HEK, CHO and FRT cells by the trypan blue exclusion staining method (Louis and Siegel, 2011). Cells were exposed to each compound for 30 minutes. After exposition, cell were trypsinized and harvested for toxicity evaluation. To avoid an underestimation of the amount of dead cells, also the cells that have been detached from the plate during the anionophore exposition were collected and considered. For each cell line (CHO, FRT and HEK293) the concentrations of each compuond that were assayed were: 10, 5, 2.5, 2, 1, 0.5, 0.25, 0.125, 0.0625 and 0 (vehicle, DMSO) μM. For each cell line and for each concentration assayed, the toxic effect of anionophores was evaluated performing the trypan blue test on 5 biological replicates. In each experiment an amount of at least 150 cells was considered. The concentration to have half of the maximum toxicity, $TD_{50}$, was calculated plotting the percentage of cell suvival against the anionophore concentration (*A*), and fitting the data with:

(1)

An assay to distinguish between healthy, early apoptotic, late apoptotic and necrotic cells (Apoptosis/Necrosis detection kitR, Enzo, Lausen, Switzerland) was applied to HEK cells treated with anionophores. HEK293 cells were exposed for 15 minutes to each compound, at a concentrations of 1.5, 0.5 0.25 or 0 μM. This assay is compatible with GFP and YFP fluorescent probes, but the fluorescence of prodigiosin and obatoclax interferes with the assay, impeding the apoptosis test with these two anionophores. The maximum inducible apoptosis $AD_{50}$, was calculated fiting the % of apoptotic cells agains the anionophore concentration with an equation similar to that used for toxicity calculations.

**Chloride efflux assay in cells**

HEK cells were grown in standard conditions (37°C, 5% $CO_2$), in DMEM medium supplemented with 2 mM L-glutamine and 10% fetal bovine serum. CHO cells were grown in standard conditions, in Ham's F12 medium supplemented with 2 mM L-glutamine and 10% fetal bovine serum. Cells at 80% confluence were detached from the bottom of the flask by soft scrapping, washed in chloride-free buffer (in mM: 136 $NaNO_3$, 3 $KNO_3$, 2 $Ca(NO_3)_2$, 20 HEPES, 11 Glucose, pH 7.4), suspended in 4 ml of chloride-free buffer (~ $15\times10^6$ cells), and used immediately. Ionophores were dissolved in **100%** DMSO to a concentration of 10 mM. The final concentration of DMSO cells were exposed was ≥0.3%. Control record were done using 0.3% DMSO. Chloride concentration in the extracellular solution was continuously measured with the chloride-sensitive electrode (Cossu et al., 2018; Hernando et al., 2018). After an initial equilibration, chloride efflux was induced by a small volume (<1%) of ionophore. The measurement was

concluded with the addition of the sodium dodecyl sulphate (SDS) at a final concentration of 1% to break off the membranes and measure the total chloride content in the cells. Experiments were done at 25 ± 1°C.

**Iodide influx assay in cells**

FRT cells stably transfected with a halide-sensitive yellow fluorescence protein (YFP-H148Q/I152L) (Galietta et al., 2001a, 2001b) cells were cultured in standard conditions (37°C, 5% $CO_2$) on black-wall, clear bottom 96-well micro-plates at a density of 40,000 cells per well in Coon's modified medium supplemented with 10% serum, 2 mM L-glutamine, 1 mg $ml^{-1}$ penicillin, 100 µg $ml^{-1}$ streptomycin, and 0.5 mg $ml^{-1}$ hygromycin as selection agent for the YFP. For some experiments, cells were stably co-transfected with the YFP and with a wild type CFTR, or CFTR carrying the cystic fibrosis mutations G551D or F508del were used. In these cases he culture medium contained 1 mg $ml^{-1}$ geneticin (G418) and 0.6 mg $ml^{-1}$ zeocin as selection agents. Functional experiments were done 48 h after cell seeding.

The activity of anionophores was determined in FRT cells expressing the halide-sensitive YFP protein, using a fluorescence plate reader (Tristar2 S, Berthold Technologies) equipped with 485 nm excitation and 535 nm emission filters, as previously described (Caci et al., 2008). The assay is based in the fact that the fluorescence of the YFP protein is quenched to a greater extend by $I^-$ than by $Cl^-$ (Galietta et al., 2001a). If not otherwise stated, 30 minutes before the assay, the cells were washed twice with a solution containing (in mM): NaCl 136, $KNO_3$ 4.5, $Ca(NO_3)_2$ 1.2, $MgSO_4$ 0.2, Glucose 5, HEPES 20, (pH 7.4). The cells were incubated in 60 µl of this solution at 37°C with anionophores or with DMSO as control.

Once the assay started, the fluorescence was recorded every 0.2 seconds for as long as 14-65 s for each well. At 5 seconds after the start of fluorescence recording were injected 100 µl of an extracellular solution containing 136 mM NaI instead of NaCl, so that the final concentration of NaI in the well is 85 mM. The iodide influx is detected as a fluorescence quenching as the anion binds to the intracellular YFP. The initial rate of fluorescence decay (*QR*) was derived by fitting the signal with a double exponential function, after background subtraction and normalization for the average fluorescence before NaI addition (Galietta et al., 2001a, 2001b; Caci et al., 2008). The *QR* is a direct indication of the activity of the tested compound.

For the pH-dependence experiments, cells were washed with a solution containing (in mM): NaCl 137, KCl 2.7, $Na_2HPO_4$ 8.1, $KH_2PO_4$ 1.5, $CaCl_2$ 1 and $MgCl_2$ 0.5 (pH 7.3). During the assay, it was injected 165 µl of an extracellular solution containing 137 mM NaI instead of NaCl, so that the final concentration of NaI in the well is 100 mM. To explore the effect of lowering the extracellular pH, the NaI solution was buffered at pH 6.9 with HEPES, or at pH 6.6 and 6.2 using MES. The YFP fluorescence plate was measured with a plate reader (FLUOstar Galaxy, BMG) equipped with 500 nm excitation and 535 nm emission filters.

**Membrane potential measurements**

Changes of the cell membrane potential were measuredin HEK cells with the fluorescence probe Bis-(1,3-Dibutylbarbituric Acid)Trimethine Oxonol ($DiBAC_4(3)$, Thermo Fisher Scientific, Rodano, Italy), with an excitation wavelength at 485 nm and emission to 520 nm. With this probe, hyperpolarization is observed as the decrease of fluorescence. HEK cells seeded on 96-well micro-plates at a density of 40,000 cells per well. Cells were incubated in 60 µl of Cl-solution (in mM: NaCl 136, $KNO_3$ 4.5, $Ca(NO_3)_2$ 1.2, $MgSO_4$ 0.2, Glucose 5, HEPES 20, pH 7.4) or in gluconate solution (Na-gluconate substituting the NaCl) with 1 µM of $DiBAC_4(3)$ dye, with or without 2 µM of anionophores, or DMSO as control (see figure S12), for 30 minutes at 37°C in agitation. The final concentration of DMSO to which cells were exposed was ≤ 0.3% in all assays, both with anionophores and pure DMSO. Cells were washed twice with 100 µl of the respective buffer, and fluorescence was measured in the plate reader. The change of the membrane potential in a given condition was expressed as the relative change of the probe $DiBAC_4(3)$ fluorescence, normalised by the fluorescence of the untreated cells, kept in normal NaCl extracellular solution, as the resting membrane potential reference ($\Delta F/F_0$).

**Bicarbonate transport in cells**

The intracellular pH ($pH_i$) was measured in FRT cells using the fluorescent pH indicator 2',7'-bis(2-carboxyethyl)-5-(and-6)carboxyfluorescein (BCECF). FRT cells, seeded on glass-bottom Petri dishes, were grow to ~80% confluence. Cells were loaded with 5 µM of BCECF acetoxymethyl ester in the culture medium without serum for 30-40 min at room temperature. Cells were washed 3 times with recording solution containing (mM): NaCl 140, $K_2HPO_4$ 2.5, $MgSO_4$ 1, $CaCl_2$ 1, HEPES 10, glucose 6 (pH 7.3), and were allowed to recover for at least 30 minutes before measurement. All used solutions were equilibrated with 5% $CO_2$ and 95% air. The Petri dish was mounted in a perfusion system in the stage of an optical instrument composed of a basic iMIC epifluorescence inverted microscope with a QImaging Retiga EXI Blue camera a (Till Photonics, Graefelfing, Germany). Cells were visualized with an Olympus Objective Plan Super Apochromat 10x (N.A. 0.4, W.D. 3.1mm). For excitation we used Till Oligochrome a wavelength-switching device containing a stable Xenon light-source. Sample was excited at two wavelenghs, 440 nm and 490 nm, and emission was recorded at 520 nm. To estimate the $pH_i$, the intracellular pH was varied incubating the cells in high potassium concentration solution with 15 µM nigericin to equilibrate external with internal pH; a calibration curve was constructed plotting the pH against the ratio of fluorescence emited upon exitation at the two excitation wavelenghts.

The transport of bicarbonate was examined measuring the changes of $pH_i$ using the $NH_4^+$ prepulse technique (Kintner et al., 2004). $NH_4^+$ solutions were prepared by replacing 20 mM NaCl in the recording solution with an equimolar concentration of $NH_4Cl$. When cells were subjected to an acid load by the transient application (2–3 min) of a 20 mM $NH_4^+$ solution $pH_i$ rose as $NH_4^+$ accumulated in the intracellular space during the prepulse. Cells were subsequently returned to a recording solution without $NH_4^+$, and acidification of the cytoplasm occurred when $NH_3$ quickly diffused out of the cell. For the extracellular bicarbonate solution, 40 mM of NaCl was substitutted by $NaHCO_3$. The $Na^+/H^+$ exchange, the $Na^+/HCO_3^-$ co-transport, the $Cl^-/HCO_3^-$ and the $Na^+$-dependent $Cl^-/HCO_3^-$ exchangers inhibition was obtained by adding 1 mM amiloride and 300 µM disodium 4,4'-Diisothiocyano-2,2'-stilbenedisulfonate (DIDS), respectively, to the recording solution (Burnham et al., 1997; Lee et al., 1999; Shumaker and Soleimani, 1999) Moreover, DIDS also inhibits the calcium-activated chloride channels bestrophin and Anoctamin 1 that both display $HCO_3^-$ permeability (Hartzell et al., 2005). Anionophores were added directly to solution to the desired concentration. Similar experiments were done also with FRT cells stable transfected with CFTR and 20 µM forskolin was added to the recording solutions to activate CFTR channels.

**Drug interaction**

FRT cells stably transfected with a halide-sensitive YFP and CFTR (wild type, or the CFTR-mutants G551D and F508del) were plated on 96-well micro-plates as described above. The iodide influx assay was used to investigate the possible anionophores interferences on the activity of drugs, potentiators and correctors, which interact with CFTR. Cells expressing wild type CFTR were incubated for 40 min with selected anionophore as control and 20 µM of forskolin to activate CFTR transport, and with or without 10 µM of the CFTR potentiator Ivacaftor. Cells expressing G551D CFTR mutant were incubated with the selected anionophore and 20 µM of Forskolin, with or without 10 µM of the CFTR potentiator Ivacaftor to activate G551D mutant (Eckford et al., 2012; Gianotti et al., 2013; Hadida et al., 2014). Cells expressing F508del mutant were incubated overnight with 5 µM of Lumacaftor (Van Goor et al., 2011; Ren et al., 2013; Loo and Clarke, 2017). For the assay, cells were incubated with 20 µM forskolin, with or without anionophores to measure anion transport. In all experiments, the vehicle DMSO was used as negative control.

**Data analysis**

The data and statistical analysis comply with the recommendations on experimental design and analysis in pharmacology (Curtis et al., 2015) Data were analysed with IgorPro 7 (Lake Oswego, Oregon, USA). All values are presented as the mean ± SEM and n representst he number of experiments. Data points were weighted by their standard deviation in the fit of concentration-response curves. Fitting results are presented ± standard deviation. Comparison between two groups and a group agaisnt a specified value was done using Student'st-test (Zar, 1999), and the *t*, probability *P* and degrees of freedom ν values are reported. All experiments were performed unblinded.

## Results

### Anionophore-driven chloride transport in vesicles

The five selected compounds, prodigiosine (PRG), obatoclax (OBX), EH130, MM3 and RQ363 were first assayed in phospholipid large unilamelar vesicles (LUV). All these compounds promote the efflux of the chloride encapsulated in LUV. In Fig 1A is displayed the time course of the normalised chloride concentration upon the addition of MM3 at concentrations from 0.005 µM to 5 µM, showing that the chloride efflux depends on the concentration of the anionophore. Application of the sole vehicle (DMSO) does not produce any chloride efflux. Application of the anionophore elicits chloride release from the interior of the vesicles, raising the external chloride concentration as detected by the chloride selective electrode. A maximum chloride concentration is obtained by lysing the vesicles upon addition of a detergent. This $Cl^-$ max value is used for normalization of the data. The initial time, $t = 0$, represents addition of the anionophore and $t = 300$ s is the arbitrary time chosen to end the experiments. The dose-response was constructed plotting the normalised chloride efflux in 300 s against the anionophore concentration, and data was fitted with the Hill's equation (Figure 1C). The same procedure was applied to each of the studied anionophores (see Supplementary Fig S7-S11), and the results of the dose-response fittings are presented in Table 1. Prodigiosin is the most potent anionophore, while its triazole derivative is about 7-fold less potent (Hernando et al., 2018). Also the two tambjamines studied has different potency, being MM3 2.5-fold more potent than RQ363 (Hernando et al., 2014b). For all anionophores the Hill's exponent is not significantly different from 1, suggesting that the molecules participate in the transport as monomers (Black and Leff, 1983; Weiss, 1997).

### Anionophore toxicicity

Toxicity data for the cell lines chinese hammster ovary (CHO), Fischer rat tyroid (FRT) and human embryonic kidney (HEK) is presented in Table 2. The concentration for 50% of the maximum toxicity, $TD_{50}$, is quite well correlated in the three cell lines, showing that OBX and PRG are the most toxic substances. As previously described, triazole derivative of prodigiosine in EH130 attenuates the cell toxicity of the anionophore (Cossu et al., 2018; Hernando et al., 2018), while the two tambjamines are significantly less toxic than prodigiosines. The concentrations to obtain the half of the maximum inducible apoptosis is also shown in Table 2. For all evaluated data, extrapolation to high anionophopre concentration idicates that would produce 100% apoptosis induction.

### Chloride efflux assay in cells

We measured the anionophore-driven chloride efflux on suspensions of HEK or CHO cells. Application of the anionophore vehicle, DMSO does not induce any measurable chloride efflux (supplementary Fig. S12). Differently, addition of the micromolar concentrations of anionophores evoke a significant efflux of chlorides in the cells, as displayed in figure 2. There, it is shown that application of EH130 (figure 2A) and MM3 (figure 2B) induces a concentration-dependent chloride efflux. Similar effect is produced when anionophores PRG, OBX and RQ363 are applied to cell suspensions (supplementary figure S12). Cell responses were similar with the two cell lines, HEK and CHO.

### Iodide influx assay in cells

The iodide influx was measured as the initial quenching rate of the fluorescence in FTR cells expressing iodide-sensitive YFP. In figure 3A is shown the time course of the fluorescence decay after addition of iodide in the extracellular solution. Control cells, treated with the vehicle DMSO showed a slow quenching rate, *QR*, consistent with the endogenous transport of iodide by FRT cells. Treatment of cells with 2 µM anionophores causes a significant increase of the rate of iodide influx, as seen in figure 3A. The *QR* is proportional to the concentration of the anionophore, as shown for MM3 in figure 3B. For comparison, supplementary figure S13 shows representative records obtained for all the anionophores studied, at two different concentrations.

Concentration-response curves for a given anionophore were constructed by plotting the average *QR* measured in 6 to 10 independent measurements at each concentration (Figure 4). The curves were well fitted with a first order receptor-binding model (Kenakin, 2010),

(2)

where *A* is the concentration of the anionophore, $EC_{50}$ is effective concentration to produce the half of the maximum effect, $QR_{max}$. The fitting results are presented in Table 3. The relative potency of the anionophores measured in cells is different as that reported for LUV measurements. The $EC_{50}$ of EH130 is not significantly different to those of the tambjamines MM3 ($t$=0.810, $P$=0.42) and RQ363 ($t$=0.225, $P$=0.82), and the most potent anionophores (with lower $ED_{50}$) are OBX and PRG. Instead, the efficacy of iodide transport, described by $QR_{max}$, shows that the tambjamine MM3 is the most effective transporter, being more than 5-fold more effective than the natural product PRG. The other two prodigiosine derived anionophores are less effective than PRG, yielding one half and one third $QR_{max}$, for OBX and EH130, respectively. The less effective anionophore is the second tambjamine studied, RQ363 (Figure 4 and table 3). It is interesting to notice that the potency ($EC_{50}$) and the efficacy ($QR_{max}$) of these anionophores are not correlated, and therefore both parameters needs to be determined in the choise of substances for an eventual therapeutic use.

**Effect of the pH**

We have previously reported that the transport efficacy of triazole derivatives of prodigiosin strongly depends on pH (Cossu et al., 2018; Hernando et al., 2018), being the ionization state of these compounds the determinant parameter for such pH dependency (Cossu et al., 2018). Thus, considering that all the anionophores studied have a protonable group involved in the chloride binding (Seganish and Davis, 2005; Díaz de Greñu et al., 2011; García-Valverde et al., 2012; Iglesias Hernández et al., 2012; Hernando et al., 2014b, 2018), with a $pK_a$ plausibly near to the physiological pH, it is expected that the transport properties of all these substances will depend on the pH.

Thus, to confirm this hypothesis, we carried out transport assays with external solutions at pH 6.2 ($n$ = 6 to 16), 6.6 ($n$ = 8 to 57), 6.9 ($n$ = 6 to 18) and 7.3 ($n$ = 11 to 63). We observed a significant increase of *QR* when the extracellular pH was set at acid values (Supplementary figure S14). In Fig 5A-E are shown the average of the *QR* measured at different pH, normalised by the *QR* measured at pH 7.3. Notice that the reduction of 1.1 pH unit increases the activity of EH130 12-fold ($t$=7.18, $P$=5.2×10$^{-5}$, ν=14), OBX 9.3-fold ($t$=7.63, $P$=5.5×10$^{-4}$, ν=67), PRG 11.9-fold ($t$=10, $P$=1.6×10$^{-4}$, ν=38), MM3 2.8-fold ($t$=14.5, $P$=1.2×10$^{-11}$, ν=34), and RQ363 7.3-fold ($t$=9.4, $P$=2.2×10$^{-8}$, ν=27). Notice that the effect is more marked for prodigiosines than for tambjamines (figure 5F).

**Anion Competition**

To compare the chloride and iodide transport efficacy of anionophores we subtituted isoosmotically chloride in the extracellular solution by gluconate. Gluconate has a radius of 3.76 Å, that is significantly larger than the chloride radius of 1.81 Å (Schlumberger et al. 2014), and transport of gluconate has been demonstrated to be virtually absent for triazole derivated prodigiosines in vesicles (Cossu et al., 2018). We hypothesized that chloride and iodide are competing for the anion carriers, thus, the substitution of chloride by gluconate will increase the iodide influx. Indeed, as expected, figure 6A (red squares) shows that reduction of chloride results in an increase of the iodide influx driven by PRG. For prodigiosines, statistical comparisons of the *QR* measured in absence of chloride (51 mM gluconate) and in 51 mM chloride (0 gluconate) yield a significant increase of iodide transport ($t$=3.61, $P$=2.2×10$^{-3}$, ν=22 for EH130, $t$=3.41, $P$=4.3×10$^{-3}$, ν=14 for OBX, $t$=2.8, $P$=0.011, ν=21 for PRG). (Figure 6B, red bars). Conversely, for the tambjamine MM3 the substitution of chloride by gluconate results in a reduction of iodide transport (Figure 6A, blue circles). In general, we observed a significant reduction of iodide transport in the tambjamines when chloride was substituted by gluconate ($t$=7.46, $P$=3.1×10$^{-6}$, ν=23 for MM3, $t$=7.97, $P$=3.8×10$^{-7}$, ν=18 for RQ363) (Figure 6B, blue bars). We hypothesize that, for the tambjamines, the increase of the gluconate concentration lead to the binding of this anion to the anionophore, forming a membrane impermeable complex, and causing a iodide transport blockage. Differently, prodigiosines do not bind gluconate, and the reduction of the concentration of chloride results on a more anion free available transporters, and therefore favours the binding, and successive transport of iodide. Representative traces of these experiments are shown in the supplementary figure S15.

**Membrane Potential**

In the presence of extracellular chloride, the vehicle DMSO does not change the cell resting potential ($t$=0.65, $P$=0.52, ν=13), as measured by the change in fluorescence ($\Delta F/F_0$) of the probe $DiBAC_4(3)$ (dark green in figure 7). The incubation of cells with 2 µM of the prodigiosines (red in figure 7) induce a significant decrease in fluorescence ($t$= 4.48, $P=1.4\times10^{-4}$, ν=26 for EH130, $t$=7.28, $P=3.2\times10^{-7}$, ν=28 for OBX, $t$=6.24 $P=1.7\times10^{-6}$, ν=29 for PRG), that is consistent with a hyperpolarization of cells. An hyperpolarization is also observed in the cells incubated with the tambjamine RQ363 ($t$=2.43, $P$=0.022, ν=26) (blue in figure 7). The extent of the hyperpolarization is correlated with the efficacy of these anionophores (see Table 3). However, the second tambjamine studied, MM3, does not induce any membrane potential change in the cells ($t$=0.07, $P$=0.94, ν=29) .

When the extracellular chloride is substituted by gluconate, the consequent intracellular chloride loss induce a cell hyperpolarization ($t$=2.53, $P=5.3\times10^{-1}$, ν=13), and the presence of the anionophores EH130, OBX, PRG and RQ363 (figure 7, light coloured columns), do not further change significantly the cell membrane potential ($t$= 0.43, $P$=0.67, ν=29 for EH130, $t$=1.27, $P$=0.22, ν=27 for OBX, $t$=1.90, $P$=0.069, ν=28 for PRG, $t$=0.16, $P$=0.87, ν=30 for RQ363), Differently, also in the presence of gluconate the anionophore MM3 does not change the membrane potential with respect of the untreated cells.

**Bicarbonate transport**

The bicarbonate transport was studied with the $NH_4^+$ pulse protocol (Kintner et al., 2004) In this protocol, there is an intracellular acidification phase at the end of the $NH_4^+$ pulse, followed by an intracellular alkalinization when $NH_4^+$ was removed and FRT cells were perfused with bicarbonate (Figure 8A). This alkalinization could be due to an influx of protons through the $Na^+/H^+$ exchange or to a bicarbonate influx through the $Na^+/HCO_3^-$ co-transport and the $Na^+$-dependent and independent $Cl^-/HCO_3^-$ exchangers. When the main bicarbonate and proton transport mechanisms were inhibited by 1 mM amiloride and 300 µM disodium-4,4'-diisothiocyano-2,2'-stilbenedisulfonate (DIDS), respectively (Burnham et al., 1997; Lee et al., 1999; Shumaker and Soleimani, 1999), the extracellular bicarbonate does not enters the cell, leaving the intracellular pH ($pH_i$) constant (Fig 8B). Under these conditions, the perfusion of FRT cells with 2 µM EH130 (Figure 8C) or 2 µM MM3 (Figure 8D), results in a rapid increase of $pH_i$, caused by the anionophore-induced bicarbonate influx. Observe that, in absence of extracellular bicarbonate, application of the anionophore does not induce any intracellular pH change (Figure 8E). Similar experiments were done on FRT cells stably transfected with CFTR (FRT-CFTR cells) (Figure 8F). Also in this case the addition of 1mM amiloride and 300 µM DIDS blocked the different bicarbonate pathways of the cells and alkalinization was observed only after the activation of CFTR by forskolin.

Application of 2 µM of EH130 ($t$=0.14, $P$=0.9, ν=8), OBX ($t$=0.91, $P$=0.41, ν=8), PRG ($t$=1.47, $P$=0.22, ν=8), and MM3 ($t$=0.47, $P$=0.66 ν=8), causes a change of $pH_i$ similar to that caused by the activation of the CFTR by 20 µM of forskolin (Figure 8G). A smaller, but still significant change of $pH_i$ is also caused by the tambjamine RQ363. In these experimental conditions, where cells are perfused with solutions equilibrated with 5% $CO_2$, and assuming that the $CO_2$ in extracellular space is in equilibrium with that of the intracellular space, it is possible to calculate the change in the intracellular concentration of bicarbonate applying the equation of Henderson-Hasselbach, as shown in the right axis in Figure 8G, indicating a net bicarbonate influx driven by the anionophores.

**Drug Interaction**

In control FRT cells transfected with CFTR, application of 20 µM forskolin elicits a iodide influx driven by the activation of the CFTR (DMSO, magenta bar in figure 9A). These cells expressing CFTR show a iodide influx when are treated with 2 µM anionophore (Figure 9A, light coloured bars), that further increase as cells are treated with forskolin (Figure 9A, strong coloured bars). Notice that the anion influx in this group of experiments are roughly the sum of the transport due to the anionophore, represented by the light coloured bars in Figure 9A, and the transport driven by the CFTR shown as a magenta bar in Figure 9A. Indeed further increase of the CFTR-mediated anion transport occurs by addition of 10 µM of the CFTR-potentiatior Ivacaftor (dashed bars in figure 9A), also in the presence of anionophores. These data provide two important outcomes: The anionophores do not appear to acutely disrupt activation of CFTR by forskolin. The second result is that anionophores does not interfere with the CFTR potentiation mechanism of the drug Ivacaftor.

Similar experiments were done with FTR cells expressing the CF-mutant G551D (Figure 9B). In these cells, stimulation of CFTR by forskolin does not elicit any anion flux, as this mutation produces a gating defect on CFTR, reducing almost completely the capacity to open the channel. This defect can partially corrected using the potentiator Ivacaftor (dashed magenta bar in figure 9B). Interestingly, an anion transport can be also restored by treatment of the mutated-CFTR cells with anionophores (light coloured bars in figure 9B), but in this case, addition of forskolin does not further increase the anion transport, as the G551D-CFTR is not functioning (strong coloured bars in figure 9B). However, when the potentiator Ivacaftor is added, it is possible to notice a further increase of iodide influx, because the addition of the anionophore-driven and the CFTR-mediated anion transport (dashed bars in figure 9B). Notice that the tambjamine MM3 is the most effective anion transporter in G551D-transfected cells.

The reduced anion transport on cells transfected with the mutant F508del can be efficiently recovered by the overnight treatment with 5 μM of the corrector Lumacaftor (strong coloured and dashed magenta bars in figure 9C). Application of anionophores produce a significant anion influx, that is further increased when CFTR is stimulated with forskolin (light and strong coloured in figure 9C). The rescue of the F508del-CFTR is evident from the dashed bars on figure 9C, were cells were treated with Lumacaftor, and incubated with the anionophore and forskolin. These data confirm that, except for OBX, there is not interaction between the action of the anionophores and the correction mechanism of Lumacaftor. It is interesting to notice that efficacy of MM3 is the highest, and the increase of flux upon forskolin application is unexpectedly high.

**Discussion**

We have studied the anion transport properties of a set of synthetic compounds, named anionophores. These substances belong to two families, the prodigiosines (PRG, OBX and EH130) and the tambjamines (MM3 and RQ363). The two groups of substances have a very similar structural motif, with three NH groups, one of them ionizable with a $pK_a$ between 6 and 7 (see figure S1 in the supplementary data). The difference between the two groups is that the ionizable NH group in the tambjamines is an imine, and in the prodigiosines is located in an azafulvene heterocycle. Solid state X-ray diffraction studies, *ab initio* theoretical calculations and NMR analysis of these compounds have demonstrated that al these molecules are capable to coordinate an anion through hydrogen bonds to the three NH groups (Díaz de Greñu et al., 2011; García-Valverde et al., 2012; Iglesias Hernández et al., 2012; Hernando et al., 2014b; Soto-Cerrato et al., 2015; Hernando et al., 2018). As reported elsewhere (Díaz de Greñu et al., 2011; Iglesias Hernández et al., 2012; Saggiomo et al., 2012; Hernando et al., 2014b; Cossu et al., 2018; Hernando et al., 2018), EH130, PRG, OBX and RQ363 are capable of exchanging chloride with nitrate across the bilayer membrane in a vesicle models (see also Supplementary Fig S7-S11). Here we report that also the tambjamine MM3 has the same anion transport properties (Figure 1B and C).

To use these substances in cells, with the expectation to employ them as therapeutic drugs, is a big challenge, since this molecules are derivatives of cytotoxic natural products. Indeed, substances like obatoclax have been proposed as antitumor chemotherapeutic (Hernando et al., 2014b; Ko et al., 2014; Rodilla et al., 2017). Indeed, an effort to reduce the prodigiosine related molecules has been successful preparing the triazole derivatives of prodigiosine (Cossu et al., 2018; Hernando et al., 2018). Now, we have used two tambjamines MM3 and RQ363, that are sensibly less toxic than the prodigiosines (Table 2), to analyse the anion transport in cells. To our knowledge, this is the first report of tambjamine-driven anion transport in living mammalian cells. These data are compared with the results obtained with prodigiosines to have a better insight on the anion transport mechanisms by these two anionophores families.

The first attempt was, indeed, to reproduce in cells the chloride efflux measurements already well standardised in unilamellar vesicles. However, even been possible to record anionophore-driven chloride effluxes (Figure 2), quantification of the records was made difficult by several technical problems. First, because the intracellular chloride concentration in epithelial cells is low, between 20 to 40 mM (Willumsen et al., 1989; Treharne et al., 2006; Bregestovski et al., 2009; Falkenberg and Jakobsson, 2010), even reducing the extracellular chloride to concentrations near to zero, the gradient is very small, and the magnitude of the efflux is consequently reduced. These conditions also influence the resolution of the measurements, as the chloride leaving the cell is further diluted in the external solution,

reaching extracellular chloride concentrations at the limit of the ion sensitive electrode resolution. On the other hand, keeping the cells in a low chloride solution, even for short periods of time, induce an intracellular chloride depletion, further reducing the chloride gradient, and causes the activation of the cell mechanisms entrusted on the ion concentration homeostasis, that in turn may interfere with our measurements of anionophore transport. Thus, we continue the experiments determining the iodide influx, by measuring the kinetics of the fluorescence quenching of iodide sensitive YFP. This method, that was originally developed to perform high-throughput screening for searching substances that could potentiate or correct the mutant CFTR, is quite well standardised (Galietta et al., 2001a, 2001b). The method has the advantage that, assuming that initially there is not iodide in the intracellular space, the iodide injection at the beginning of the assay represents a constant iodide gradient, and therefore the initial quenching rate will be directly proportional to the iodide permeability. Thus, we could measure the anion influx driven by different anionophores just analysing the fluorescence quenching curves (Figure 3A), and study the concentration dependence of the transport activity of different anionophores (Figure 3B). With this procedure we could construct the concentration-response curves for all the studied anionophores (Figure 4), and fit them with a first order ligand-receptor model, that yields the potency of the anionophores, in terms of $EC_{50}$, and the efficacy, expressed as the maximum quenching rate, $QR_{max}$ (Table 3).

The chloride transport in mammalian cells was further confirmed by the measurement of the relative membrane potential using fluorescence probes (Figure 7). When an anionophore is applied, it results on a hyperpolarization of the cell, consistent with a chloride influx. Substituting the extracellular chloride by gluconate induce a hyperpolarization, and probably a cell chloride loss, and not further potential changes occurs when anionophores are added. Surprisingly, the membrane potential behaviour in the presence of the tambjamine MM3 is completely different. This anionophore seems to not cause any membrane potential change, even been the most effective transporter of the studied series, and further studies are needed to more thoroughly investigate this observation.

Bicarbonate transport is a mandatory attribute to include when designing a substitutive therapy molecules for CF. Indeed, in CF subjects and animal models there is a significantly reduced bicarbonate concentration, as well as lower pH, in the airway surface liquid (Quinton, 1999, 2008; Ostedgaard et al., 2011; Pezzulo et al., 2012; Abou Alaiwa et al., 2014). This situation compromise the post-secretory MUC5AC and MUC5B processes, resulting in an increased mucus viscosity (Quinton, 2008; Tang et al., 2016; Abdullah et al., 2017). We have evaluated the bicarbonate transport as the modification of the intracellular pH in conditions of controlled $CO_2$, and suppressing the most important cellular bicarbonate and proton transporters. Our data show that all the studied anionophores are capable to transport bicarbonate into cells, restoring the intracellular bicarbonate to the same values obtained by the stimulation of CFTR, except for RQ363, that has a lower bicarbonate transport capability.

The transport activity of these ionophores augment as the pH become more acid (Figure 5). This effect is due to the presence of an ionizable group in the molecule, as these anionophores are active in their protonated form (Cossu et al., 2018). This sensitivity is more prominent for the prodigiosines than the tambjamines (Figure 5F), as the main difference between these two anionophore families is the type of ionizable NH (an azafulvene in the prodigiosines and an imine in the tambjamines). However, it can be ascribed also to a putative structural difference in the structure of their anion binding site. This difference in the anion binding site was further revealed in the anion substitution experiments (Figure 6). When measuring the iodide influx in the prodigiosines, the substitution of the extracellular chloride by the gluconate causes an increase of up to 1.5-fold iodide transport. I would occur because, as gluconate does not bind the prodigiosines, the chloride and iodide compete for the binding site of the anionophore, and removal of chloride leave more molecules free to transport iodide. Differently, when chloride is substituted by gluconate there is a reduction of tambjamine-driven iodide influx by about one half. This paradoxical difference can be justified if gluconate is able to bind the tambjamine binding site, perhaps more tightly than chloride, and competing with iodide for the anionophores, decreasing the availability of tambjamines to bind iodide, and consequently reducing the flux. These data clearly demonstrate the interaction of various anions with the prodigiosines and the tambjamines is different, perhaps indicating the differences in the fine structure of the anion binding site.

The estimated anion transport carried by the CFTR, expressed as the *QR* measured after stimulation of the WT-CFTR with 20 μM forskolin, was 65.1 $ms^{-1}$ (Figure 9A). However, it should be noted that the activity of the WT-CFTR

measured as short-circuit current on FRT epithelia stably transfected with CFTR is much higher (10.6 times) than CFTR endogenously expressed in primary human bronchial epithelia (Pedemonte et al., 2010). Thus, a heuristic goal for the anionophores would be to achieve a transport equivalent to a *QR* of 6.3 $ms^{-1}$. The concentration of anionophores to produce this transport rate calculated from the data on Table 3 is, in most cases, below the micromolar concentration (0.86 µM, 0.17 µM, 0.13 µM, 0.054 µM, and 1.65 µM, for EH130, OBX, PRG, MM3 and RQ363, respectively). Notice that these concentrations are, at least, one order of magnitude below the $TD_{50}$ measured for the three cell lines (see Table 2). To further restrict the toxicology requirements, we compare the concentration needed to obtain the target *QR* of 6.3 $ms^{-1}$ with the anionophore concentration for 99% of cell survival, $TD_1$. None of the prodigiosines conform to this additional restriction, as the $TD_1$ for EH130, OBX and PRG are 9.5, 4 and 3.4 times higher than the concentration for the target *QR*. Because its low efficacy, the concentration of the tambjamine RQ363 for the target *QR* is 7.4 times the $TD_1$. Conversely, the high efficacy of the tambjamine MM3 results in a very low concentration for the target *QR*, that is 0.24 the $TD_1$.

Finally, we verified whether anionophores interferes with the activation of the CFTR by forskolin, or if anionophores can be affected, or to be modified, by the presence of the CFTR potentiator Ivacaftor, and the CFTR-corrector Lumacaftor. Measurements in cells expressing WT-CFTR have shown that the iodide influx promoted by the anionophores is roughly additive to that driven by the CFTR (Figure 9A). An increase of the CFTR activity by Ivacaftor is further added, indicating that anionophores do not interfere with the potentiator action. This important fact is confirmed by the results obtained in FRT cells expressing G551D-CFTR (Figure 9B), were the anion transport resulted by rescue of the mutated-CFTR activity by Ivacaftor is added to that driven by ionophores. Similar result are also obtained in the mutant F508del (Figure 9C). The small anion transport, resulted by severely reduced F508del-CFTR activity, is apparently recovered by the anioniophore driven transport. When the F508del-CFTR is rescued by the corrector Lumacaftor, the restored CFTR activity is added to that of the anionophores.

~~Here we have complemented the data previously reported (Cossu et al., 2018; Hernando et al., 2018), extending the data to other prodigiosines and tambjamines.~~ The experiments demonstrate that these anionophores could be used to promote chloride and bicarbonate transport in cells, i.e., are good candidates to replace the defective or missing CFTR in an attempt to design a new cystic fibrosis therapy, as proposed for other anion transporters (Shen et al., 2012; Valkenier et al., 2014; Li et al., 2016; Liu et al., 2016; Dias et al., 2018). The analysis of anionophore-induced anion transport in cells needs, in any case, to be extended, exploring the long-lasting effects of the anionophore treatment in cells, and studying the anionophore-induced ion transport in epithelial models, where the polarization of cells plays a fundamental role on the directionality of ion transport, to find the best suited compounds to become candidates for cystic fibrosis therapy. These data represent an encouraging promise for future developments toward a mutant-independent cystic fibrosis therapy.

**Conclusions**

We have shown that the two anionophore groups studied here are able to transport halides and bicarbonate in mammalian cells, with a quantitatively similar efficiency of the native CFTR, opening the possibility to propose a CF therapy based on a substitutive transport mechanism. The transport efficacy of these anionophores is high enough to hypothesize their use at concentration significantly lower than the citotoxic concentrations. Perhaps the two prodigiosines, PRG and OBX, which have been described also as apoptosis promoters (Díaz de Greñu et al., 2011; Hosseini et al., 2013), are not appropriate for continuing these studies, but the others, in particular MM3, are very good candidates for further analysis, and for the improvement of the molecule properties. The definite prove of concept to drive the research of better, less toxic and more efficient molecules will came from further studies in a complex cellular system, as bronchial and epithelial models, where the cell polarization defines more precisely the transport characteristics of the cells, near to the physiological, and physiopathological, systems. Overall, these results represent an encouraging promise for future developments toward a mutant-independent cystic fibrosis therapy.

**Acknowledgements**. This has received funding from the European Union's Horizon 2020 research and innovation programme under grant agreement No. 667079.

**Author contributions:** O.M. and M.F. designed the experiments. R.Q., M.M. and I.C.-B. synthesized the compounds M.F., R.Q., M.M., I.C.-B., A.L., V.C., C.P., E.C. and D.B. performed the experiments and data analysis. O.M. wrote the manuscript. O.M., R.Q. and E.C. have full access to all the data int he study and takes responsibility for the integrity of the data and the accuracy of the data analysis.

**Competing Interests:** The authors declare no competing interests.

**References**


Abdullah, L.H., Evans, J.R., Wang, T.T., Ford, A.A., Makhov, A.M., Nguyen, K., et al. (2017). Defective postsecretory maturation of MUC5B mucin in cystic fibrosis airways. JCI Insight *2*: e89752.

Abou Alaiwa, M.H., Beer, A.M., Pezzulo, A.A., Launspach, J.L., Horan, R.A., Stoltz, D.A., et al. (2014). Neonates with cystic fibrosis have a reduced nasal liquid pH; a small pilot study. J. Cyst. Fibros. *13*: 373–377.

Black, J.W., and Leff, P. (1983). Operational models of pharmacological agonism. Proc R Soc Lond B Biol Sci *220*: 141–162.

Bobadilla, J.L., Macek, M.J., Fine, J.P., and Farrell, P.M. (2002). Cystic fibrosis: a worldwide analysis of CFTR mutations-correlation with incidence data and application to screening. Hum Mutat *19*: 575–606.

Boyle, M.P., Bell, S.C., Konstan, M.W., McColley, S.A., Rowe, S.M., Rietschel, E., et al. (2014). A CFTR corrector (lumacaftor) and a CFTR potentiator (ivacaftor) for treatment of patients with cystic fibrosis who have a phe508del CFTR mutation: a phase 2 randomised controlled trial. Lancet Respir Med *2*: 527–538.

Bregestovski, P., Waseem, T., and Mukhtarov, M. (2009). Genetically encoded optical sensors for monitoring of intracellular chloride and chloride-selective channel activity. Front Mol Neurosci *2*: 15.

Burnham, C.E., Amlal, H., Wang, Z., Shull, G.E., and Soleimani, M. (1997). Cloning and functional expression of a human kidney Na+:HCO3- cotransporter. J. Biol. Chem. *272*: 19111–19114.

Caci, E., Caputo, A., Hinzpeter, A., Arous, N., Fanen, P., Sonawane, N., et al. (2008). Evidence for direct CFTR inhibition by CFTR(inh)-172 based on Arg347 mutagenesis. Biochem J *413*: 135–42.

Castellani, C., and Assael, B.M. (2017). Cystic fibrosis: a clinical view. Cell. Mol. Life Sci. *74*: 129–140.

Clancy, J.P., Rowe, S.M., Accurso, F.J., Aitken, M.L., Amin, R.S., Ashlock, M.A., et al. (2012). Results of a phase IIa study of VX-809, an investigational CFTR corrector compound, in subjects with cystic fibrosis homozygous for the F508del-CFTR mutation. Thorax *67*: 12–18.

Cossu, C., Fiore, M., Baroni, D., Capurro, V., Caci, E., Magaval@ubu. Es, M., et al. (2018). Anion-transport mechanism of a triazole- bearing derivative of prodigiosine: a candidate for cystic fibrosis therapy. Front. Pharmacol. *9*:.

Curtis, M.J., Bond, R.A., Spina, D., Ahluwalia, A., Alexander, S.P.A., Giembycz, M.A., et al. (2015). Experimental design and analysis and their reporting: new guidance for publication in BJP. Br. J. Pharmacol. *172*: 3461–3471.

Davies, J.C., Moskowitz, S.M., Brown, C., Horsley, A., Mall, M.A., McKone, E.F., et al. (2018). VX-659-Tezacaftor-Ivacaftor in Patients with Cystic Fibrosis and One or Two Phe508del Alleles. N. Engl. J. Med. *379*: 1599–1611.

Davis, J.T., Okunola, O., and Quesada, R. (2010). Recent advances in the transmembrane transport of anions. Chem Soc Rev *39*: 3843–3862.

De Boeck, K., and Davies, J.C. (2017). Where are we with transformational therapies for patients with cystic fibrosis? Curr Opin Pharmacol *34*: 70–75.

Dias, C.M., Li, H., Valkenier, H., Karagiannidis, L.E., Gale, P.A., Sheppard, D.N., et al. (2018). Anion transport by ortho-phenylene bis-ureas across cell and vesicle membranes. Org. Biomol. Chem. *16*: 1083–1087.

Díaz de Greñu, B., Iglesias Hernández, P., Espona, M., Quiñonero, D., Light, M.E., Torroba, T., et al. (2011). Synthetic prodiginine obatoclax (GX15-070) and related analogues: anion binding, transmembrane transport, and cytotoxicity properties. Chemistry *17*: 14074–83.

Eckford, P.D.W., Li, C., Ramjeesingh, M., and Bear, C.E. (2012). Cystic fibrosis transmembrane conductance regulator (CFTR) potentiator VX-770 (ivacaftor) opens the defective channel gate of mutant CFTR in a phosphorylation-dependent but ATP-independent manner. J. Biol. Chem. *287*: 36639–36649.

Falkenberg, C.V., and Jakobsson, E. (2010). A biophysical model for integration of electrical, osmotic, and pH regulation in the human bronchial epithelium. Biophys. J. *98*: 1476–1485.

Galietta, L., Haggie, P., and Verkman, A. (2001a). Green fluorescent protein-based halide indicators with improved chloride and iodide affinities. FEBS Lett *499*: 220–224.

Galietta, L.J.V. (2013). Managing the underlying cause of cystic fibrosis: a future role for potentiators and correctors. Paediatr Drugs *15*: 393–402.

Galietta, L.V., Jayaraman, S., and Verkman, A.S. (2001b). Cell-based assay for high-throughput quantitative screening of CFTR chloride transport agonists. Am J Physiol Cell Physiol *281*: C1734–42.

García-Valverde, M., Alfonso, I., Quiñonero, D., and Quesada, R. (2012). Conformational analysis of a model synthetic prodiginine. J. Org. Chem. *77*: 6538–6544.

Gianotti, A., Melani, R., Caci, E., Sondo, E., Ravazzolo, R., Galietta, L.J.V., et al. (2013). Epithelial sodium channel silencing as a strategy to correct the airway surface fluid deficit in cystic fibrosis. Am J Respir Cell Mol Biol *49*: 445–52.

Hadida, S., Van Goor, F., Zhou, J., Arumugam, V., McCartney, J., Hazlewood, A., et al. (2014). Discovery of N-(2,4-di-tert-butyl-5-hydroxyphenyl)-4-oxo-1,4-dihydroquinoline-3-carboxamide (VX-770, ivacaftor), a potent and orally bioavailable CFTR potentiator. J. Med. Chem. *57*: 9776–9795.

Hartzell, C., Putzier, I., and Arreola, J. (2005). Calcium-activated chloride channels. Annu. Rev. Physiol. *67*: 719–758.

Hernando, E., Capurro, V., Cossu, C., Fiore, M., García-Valverde, M., Soto-Cerrato, V., et al. (2018). Small molecule anionophores promote transmembrane anion permeation matching CFTR activity. Sci Rep *8*: 2608.

Hernando, E., Soto-Cerrato, V., Cortés-Arroyo, S., Pérez-Tomás, R., and Quesada, R. (2014a). Transmembrane anion transport and cytotoxicity of synthetic tambjamine analogs. Org Biomol Chem *12*: 1771–8.

Hernando, E., Soto-Cerrato, V., Cortés-Arroyo, S., Pérez-Tomás, R., and Quesada, R. (2014b). Transmembrane anion transport and cytotoxicity of synthetic tambjamine analogs. Org. Biomol. Chem. *12*: 1771–1778.

Hosseini, A., Espona-Fiedler, M., Soto-Cerrato, V., Quesada, R., Pérez-Tomás, R., and Guallar, V. (2013). Molecular interactions of prodiginines with the BH3 domain of anti-apoptotic Bcl-2 family members. PLoS ONE *8*: e57562.

Hudock, K.M., and Clancy, J.P. (2017). An update on new and emerging therapies for cystic fibrosis. Expert Opin Emerg Drugs *22*: 331–346.

Iglesias Hernández, P., Moreno, D., Javier, A.A., Torroba, T., Pérez-Tomás, R., and Quesada, R. (2012). Tambjamine alkaloids and related synthetic analogs: efficient transmembrane anion transporters. Chem. Commun. (Camb.) *48*: 1556–1558.

Kenakin, T.P. (2010). A Pharmacology Primer: Theory, Applications, and Methods (Elsevier).

Kintner, D.B., Su, G., Lenart, B., Ballard, A.J., Meyer, J.W., Ng, L.L., et al. (2004). Increased tolerance to oxygen and glucose deprivation in astrocytes from Na(+)/H(+) exchanger isoform 1 null mice. Am. J. Physiol., Cell Physiol. *287*: C12-21.

Ko, S.-K., Kim, S.K., Share, A., Lynch, V.M., Park, J., Namkung, W., et al. (2014). Synthetic ion transporters can induce apoptosis by facilitating chloride anion transport into cells. Nat Chem *6*: 885–892.

Lee, M.G., Wigley, W.C., Zeng, W., Noel, L.E., Marino, C.R., Thomas, P.J., et al. (1999). Regulation of Cl-/ HCO3- exchange by cystic fibrosis transmembrane conductance regulator expressed in NIH 3T3 and HEK 293 cells. J. Biol. Chem. *274*: 3414–3421.

Li, H., Salomon, J.J., Sheppard, D.N., Mall, M.A., and Galietta, L.J. (2017). Bypassing CFTR dysfunction in cystic fibrosis with alternative pathways for anion transport. Curr Opin Pharmacol *34*: 91–97.

Li, H., Valkenier, H., Judd, L.W., Brotherhood, P.R., Hussain, S., Cooper, J.A., et al. (2016). Efficient, non-toxic anion transport by synthetic carriers in cells and epithelia. Nat Chem *8*: 24–32.

Liu, P.-Y., Li, S.-T., Shen, F.-F., Ko, W.-H., Yao, X.-Q., and Yang, D. (2016). A small synthetic molecule functions as a chloride-bicarbonate dual-transporter and induces chloride secretion in cells. Chem. Commun. (Camb.) *52*: 7380–7383.

Loo, T.W., and Clarke, D.M. (2017). Corrector VX-809 promotes interactions between cytoplasmic loop one and the first nucleotide-binding domain of CFTR. Biochem. Pharmacol. *136*: 24–31.

Louis, K.S., and Siegel, A.C. (2011). Cell viability analysis using trypan blue: manual and automated methods. Methods Mol. Biol. *740*: 7–12.

Ostedgaard, L.S., Meyerholz, D.K., Chen, J.-H., Pezzulo, A.A., Karp, P.H., Rokhlina, T., et al. (2011). The ΔF508 mutation causes CFTR misprocessing and cystic fibrosis-like disease in pigs. Sci Transl Med *3*: 74ra24.

Pedemonte, N., Tomati, V., Sondo, E., and Galietta, L.J.V. (2010). Influence of cell background on pharmacological rescue of mutant CFTR. Am. J. Physiol., Cell Physiol. *298*: C866-874.

Pezzulo, A.A., Tang, X.X., Hoegger, M.J., Abou Alaiwa, M.H., Ramachandran, S., Moninger, T.O., et al. (2012). Reduced airway surface pH impairs bacterial killing in the porcine cystic fibrosis lung. Nature *487*: 109–113.

Quinton, P.M. (1999). Physiological basis of cystic fibrosis: a historical perspective. Physiol Rev *79*: S3–S22.

Quinton, P.M. (2008). Cystic fibrosis: impaired bicarbonate secretion and mucoviscidosis. Lancet *372*: 415–417.

Ramsey, B.W., Davies, J., McElvaney, N.G., Tullis, E., Bell, S.C., Dřevínek, P., et al. (2011). A CFTR potentiator in patients with cystic fibrosis and the G551D mutation. N. Engl. J. Med. *365*: 1663–1672.

Rapoport, H., and Holden, K.G. (1962). The Synthesis of Prodigiosin. J. Am. Chem. Soc. *84*: 635–642.

Ren, H.Y., Grove, D.E., De La Rosa, O., Houck, S.A., Sopha, P., Van Goor, F., et al. (2013). VX-809 corrects folding defects in cystic fibrosis transmembrane conductance regulator protein through action on membrane-spanning domain 1. Mol Biol Cell *24*: 3016–24.

Rodilla, A.M., Korrodi-Gregório, L., Hernando, E., Manuel-Manresa, P., Quesada, R., Pérez-Tomás, R., et al. (2017). Synthetic tambjamine analogues induce mitochondrial swelling and lysosomal dysfunction leading to autophagy blockade and necrotic cell death in lung cancer. Biochem. Pharmacol. *126*: 23–33.

Saggiomo, V., Otto, S., Marques, I., Félix, V., Torroba, T., and Quesada, R. (2012). The role of lipophilicity in transmembrane anion transport. Chem. Commun. (Camb.) *48*: 5274–5276.

Schlumberger, S., Kristan, K.Č., Ota, K., Frangež, R., Molgó, J., Sepčić, K., et al. (2014). Permeability characteristics of cell-membrane pores induced by ostreolysin A/pleurotolysin B, binary pore-forming proteins from the oyster mushroom. FEBS Lett. *588*: 35–40.

Seganish, J.L., and Davis, J.T. (2005). Prodigiosin is a chloride carrier that can function as an anion exchanger. Chem. Commun. (Camb.) *0*: 5781–5783.

Shen, B., Li, X., Wang, F., Yao, X., and Yang, D. (2012). A synthetic chloride channel restores chloride conductance in human cystic fibrosis epithelial cells. PLoS ONE *7*: e34694.

Shumaker, H., and Soleimani, M. (1999). CFTR upregulates the expression of the basolateral Na(+)-K(+)-2Cl(-) cotransporter in cultured pancreatic duct cells. Am. J. Physiol. *277*: C1100-1110.

Soto-Cerrato, V., Manuel-Manresa, P., Hernando, E., Calabuig-Fariñas, S., Martínez-Romero, A., Fernández-Dueñas, V., et al. (2015). Facilitated Anion Transport Induces Hyperpolarization of the Cell Membrane That Triggers Differentiation and Cell Death in Cancer Stem Cells. J. Am. Chem. Soc. *137*: 15892–15898.

Strausbaugh, S.D., and Davis, P.B. (2007). Cystic fibrosis: a review of epidemiology and pathobiology. Clin. Chest Med. *28*: 279–288.

Tang, X.X., Ostedgaard, L.S., Hoegger, M.J., Moninger, T.O., Karp, P.H., McMenimen, J.D., et al. (2016). Acidic pH increases airway surface liquid viscosity in cystic fibrosis. J. Clin. Invest. *126*: 879–891.

Treharne, K.J., Crawford, R.M., and Mehta, A. (2006). CFTR, chloride concentration and cell volume: could mammalian protein histidine phosphorylation play a latent role? Exp. Physiol. *91*: 131–139.

Valkenier, H., Judd, L.W., Li, H., Hussain, S., Sheppard, D.N., and Davis, A.P. (2014). Preorganized bis-thioureas as powerful anion carriers: chloride transport by single molecules in large unilamellar vesicles. J Am Chem Soc *136*: 12507–12.

Van Goor, F., Hadida, S., Grootenhuis, P.D.J., Burton, B., Stack, J.H., Straley, K.S., et al. (2011). Correction of the F508del-CFTR protein processing defect in vitro by the investigational drug VX-809. Proc. Natl. Acad. Sci. U.S.A. *108*: 18843–18848.

Wainwright, C.E., Elborn, J.S., Ramsey, B.W., Marigowda, G., Huang, X., Cipolli, M., et al. (2015). Lumacaftor-Ivacaftor in Patients with Cystic Fibrosis Homozygous for Phe508del CFTR. N. Engl. J. Med. *373*: 220–231.

Weiss, J.N. (1997). The Hill equation revisited: uses and misuses. FASEB J. *11*: 835–841.

Willumsen, N.J., Davis, C.W., and Boucher, R.C. (1989). Intracellular Cl- activity and cellular Cl- pathways in cultured human airway epithelium. Am. J. Physiol. *256*: C1033-1044.

Wu, X., Judd, L.W., Howe, E.N.W., Withecombe, A.M., Soto-Cerrato, V., Li, H., et al. (2016). Nonprotonophoric Electrogenic Cl− Transport Mediated by Valinomycin-like Carriers. Chem *1*: 127–146.

Zar, J.H. (1999). Biostatistical Analysis (Englewood Cliffs, New Jersey: Prentice Hall).

Zegarra-Moran, O., and Galietta, L.J.V. (2017). CFTR pharmacology. Cell. Mol. Life Sci. *74*: 117–128.

**Table 1** Relative potencies of the anionophores measured as a normalised chloride efflux in 300 s.

| Compound | $EC_{50}$ (nM) | α |
|---|---|---|
| EH130 | 18.2 ± 1 | 1.17 ± 0.08 |
| Obatoclax | 9.7 ± 0.3 | 1.21 ± 0.06 |
| Prodigiosin | 2.5 ± 0.03 | 1.1 ± 0.11 |
| MM3 | 8.3 ± 0.7 | 1.2 ± 0.012 |
| RQ363 | 21.4 ± 9 | 0.9 ± 0.3 |

$EC_{50}$ is the concentration for 50% of the maximum efflux, and $\alpha$ is the Hill's exponent of the dose-response curve.

**Table 2** Cell viability evaluation of anionophores with the trypan blue exclusion test.

| Compound | CHO | FRT | HEK | |
|---|---|---|---|---|
| | $TD_{50}$ (µM) | $TD_{50}$ (µM) | $TD_{50}$ (µM) | $AD_{50}$ (µM) |
| EH130 | 8.0 ± 0.6 | 9.0 ± 1.1 | 6.2 ± 0.4 | 2.4 ± 0.1 |
| Obatoclax | 5.6 ± 0.6 | 4.1 ± 0.6 | 3.7 ± 0.4 | – |
| Prodigiosin | 7.0 ± 0.6 | 3.9 ± 0.8 | 2.9 ± 0.34 | – |
| MM3 | 16.8 ± 2.1 | 22.2 ± 4.4 | 24.7 ± 3.2 | 3.7 ± 0.9 |
| RQ363 | 18.0 ± 3.2 | 22.2 ± 3.0 | 17.1 ± 1.2 | 12.6 ± 0.6 |

$TD_{50}$ (± SEM) is the concentration for 50% of the maximum toxicity. The concentration for the 50% of maximum inducible apoptosis is $AD_{50}$.

**Table 3**. Effective concentration to produce the half of the maximum transport, measuring as the initial quenching rate, $EC_{50}$, and maximum effect $QR_{max}$. estimated from the fit of data presented in figure 4 with equation 2. PCC is the Pearson's correlation coefficient, and the number of data pairs is shown in parenthesis.

| Compound | $EC_{50}$ (µM) | $QR_{max}$ (1/µs) | PCC |
|---|---|---|---|
| EH130 | 2.2 ± 1.1 | 22.4 ± 1.1 | 0.904 (56) |
| Obatoclax | 0.7 ± 0.1 | 32.7 ± 1.2 | 0.808 (64) |

| | | | |
|---|---|---|---|
| Prodigiosin | 1.2 ± 0.1 | 63.0 ± 1.7 | 0.862 (63) |
| MM3 | 2.8 ± 0.6 | 334.9 ± 35.8 | 0.948 (49) |
| RQ363 | 2.4 ± 0.8 | 15.9 ± 1.4 | 0.860 (51) |

**Captions to the figures**

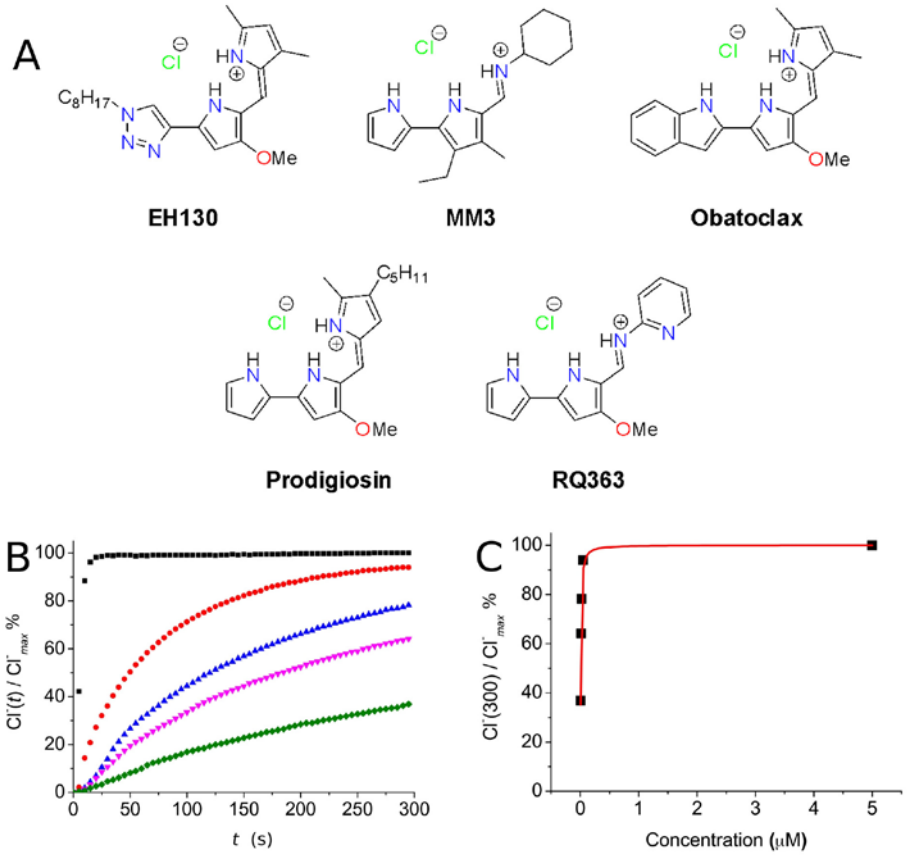


**Figure 1 A:** Chemcal structure of the studied compounds. **B:** Chloride efflux promoted by MM3 at different concentrations (5 uM, black; 0.05 uM, red; 0.025 uM, blue; 0.015 uM, magenta; 0.005 uM, green) in LUV. Vesicles loaded with 489 mM NaCl were buffered at pH 7.2 with 5 mM phosphate and dispersed in 489 mM $NaNO_3$ buffered at pH 7.2. Each trace represents the average of three independent measurements. **C:** The normalised chloride efflux at 300 s plotted against the anionophore concentration. The dose-response curve was constructed from 15 independent measurements. Data have been fitted with Hill equation (continuous line), which yields an $EC_{50}$ of 0.0083 μM.

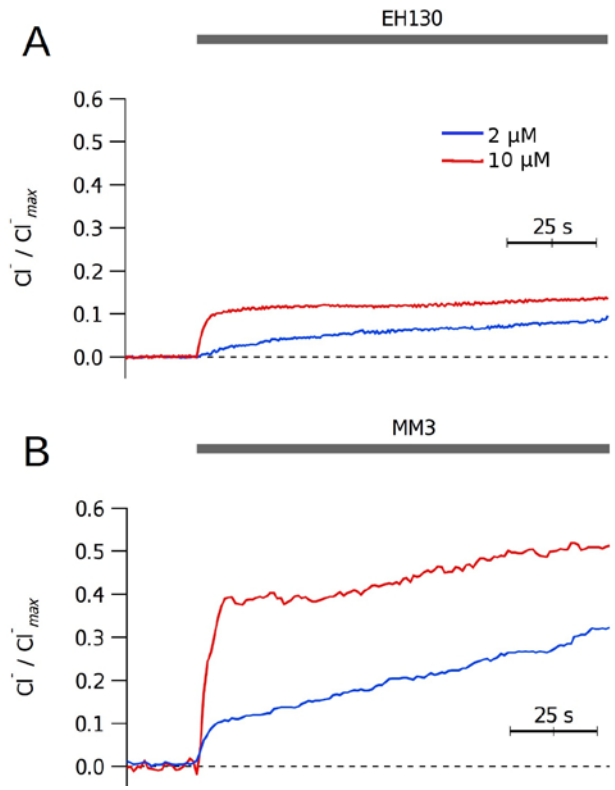


**Figure 2** Chloride efflux measured in CHO cells upon addition of different concentrations of EH130 (**A**) and MM3 (**B**). The application of 2 µM (blue trace) or 10 µM (red trace) of the anionophores are indicated by the upper bar.

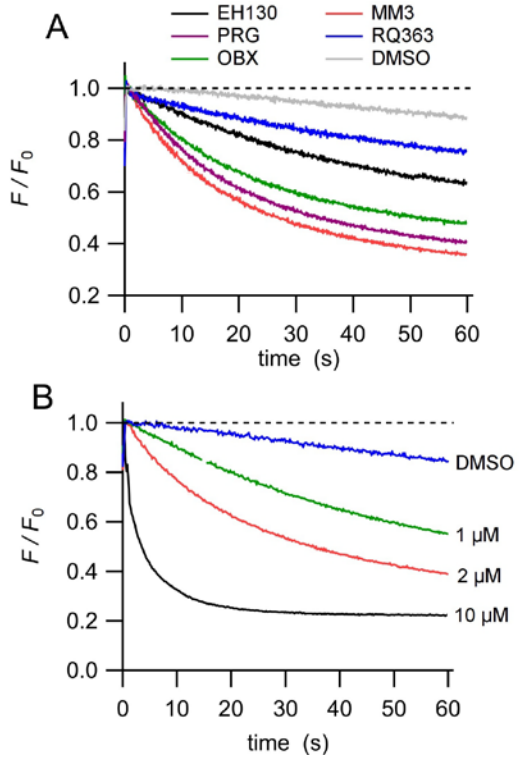


**Figure 3** Iodide influx assay in FRT cells. The fluorescence is normalised to the initial value obtained after the addition of iodide. **A:** YFP fluorescence decay by iodide influx upon addition of 2 µM of different anionophores, as indicated in the figure. Cells treated with DMSO were used as control. **B**: The time course of the fluorescence decay in cells incubated at different concentration of the anionophore MM3, as indicated in the figure.

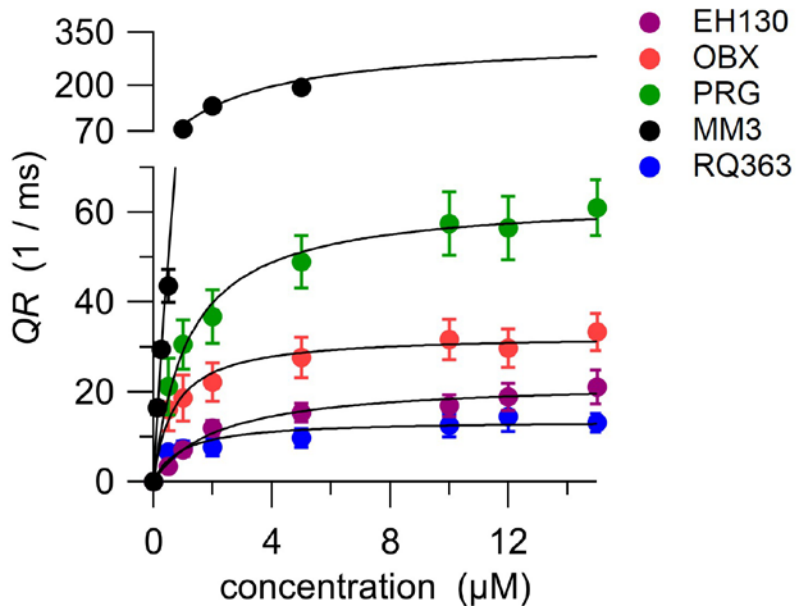


**Figure 4** The initial quenching rate (*QR*) of the YFP, indicating the iodide influx, is plotted against the concentration for the five studied compounds, as indicated on the figure. Each point represents the average of 6 to 10 different measurements, and the bars are the SEM of each measurement. The concentration-response curves, fitted with a Langmuir model (equation 2), are represented as continuous lines. Fitting results are presented in Table 3.

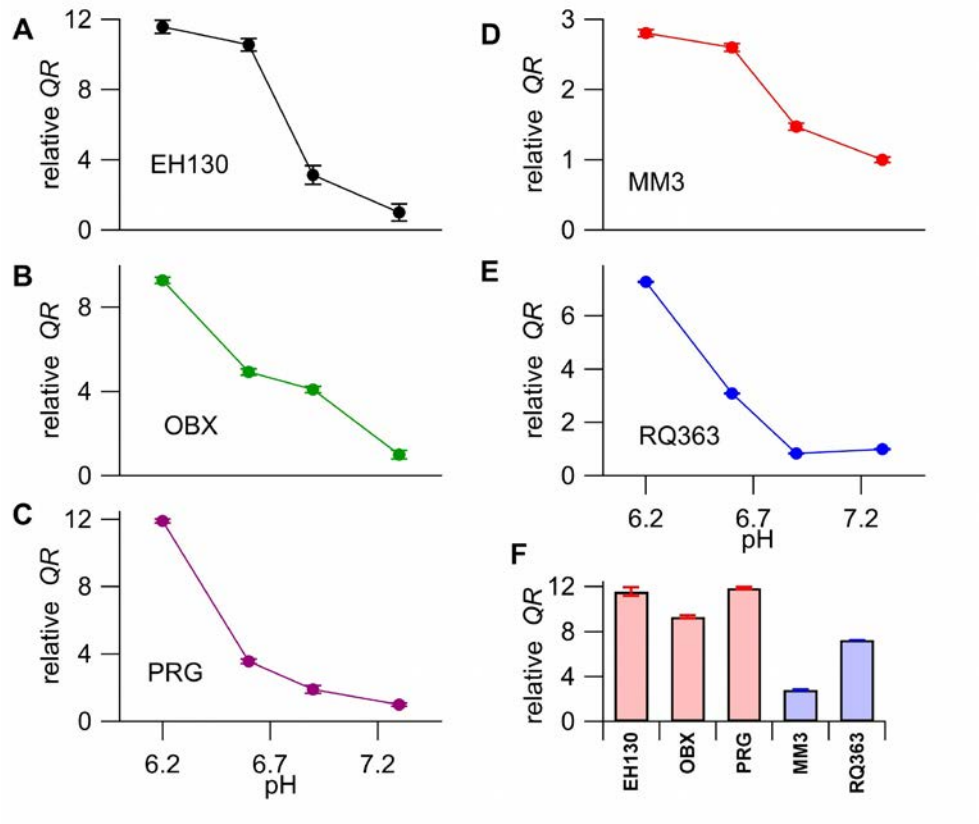


**Figure 5** The *QR* normalised by that measured at pH 7.3, are plotted against the pH of the extracellular solution, for 2 µM of EH130 (**A**), OBX (**B**), PRG (**C**), MM3 (**D**), and RQ363 (**E**). The abscissa of panels **A** and **B** are the same as panel **C**, and the abscissa of panel **D** is the same as that of panel **E**. The number of measures for each anionophore at a given pH value was between 6 and 61. The normalised *QR*, showing the change produced by the reduction of pH from 7.3 to 6.2 is shown in **F.** There, the bars representing prodigiosines are depicted in red, and those for tambjamines are in blue.

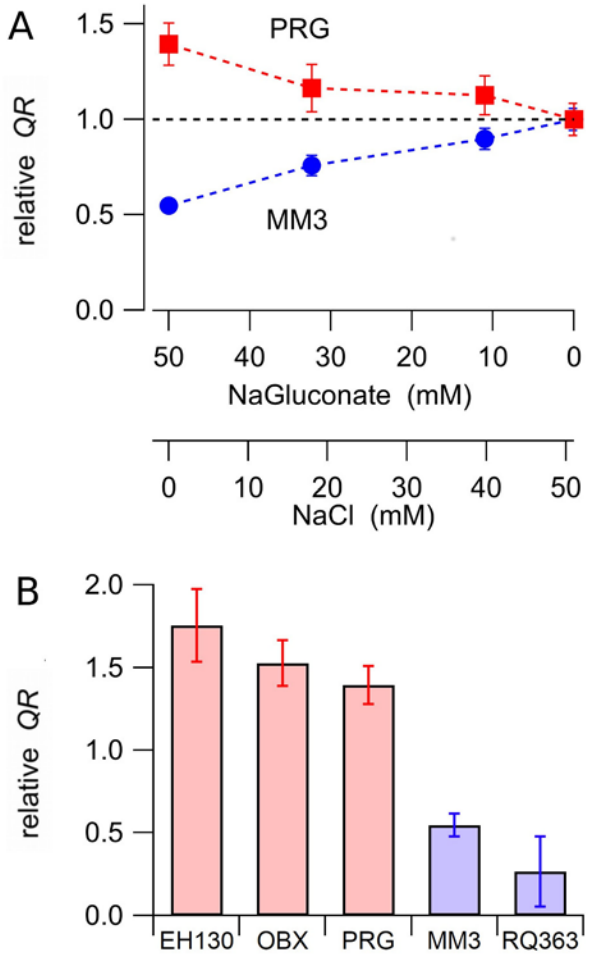


**Figure 6** Effects of anion competition in iodide transport. **A**: Iodide transport driven by PRG (red) and MM3 (blue) were measured with different concentrations of chloride and gluconate in the extracellular solution, as indicated in the two bottom axes. The relative *QR* represents the iodide influx measured at each of the chloride and gluconate combination, and was normalised by the *QR* measured with 51 mM chloride (0 gluconate). **B**: Comparison of the iodide transport measured in gluconate and in chloride, expressed as the relative *QR* in absence of chloride (and 51 mM gluconate) normalised by the *QR* measured at 50 mM chloride (and 0 gluconate). Red bars represent the prodigiosines, and blue bars the tambjamines. Data is the average of 6 to 13 measurements, and error bars are the SEM.

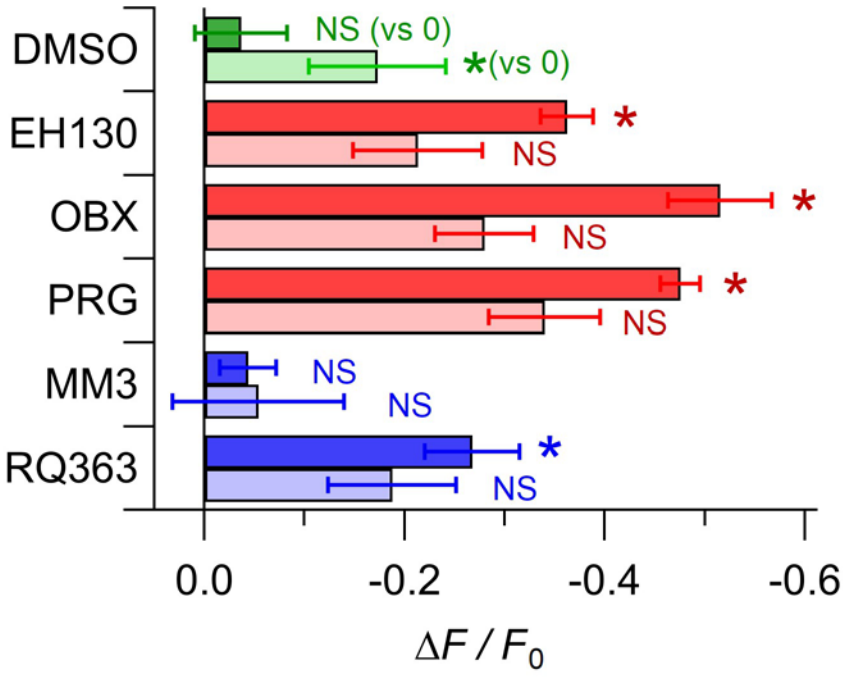


**Figure 7** Relative change of the probe DiBAC4(3) fluorescence, normalised by the fluorescence of the untreated cells, measured in control cells treated with DMSO, and in cells incubated with 2 µM of diffrerent anionophores. The dark coloured bars indicate that the extracellular solution contained chloride, and the light coloured bars indicate the substitution by gluconate. Values represent the average of, at least 10 independent measurements, and the error bars are the standard error of the mean. The DMSO controls (green) were compared to the zero value; data from cells treated with anionophores in the chloride solution (dark colored bars) were compared with data from DMSO in chloride solution treated cells, and data from cells treated with anionophores in the gluconate solution (light colored bars) were compared with data from DMSO in gluconate solution. Comparisons were done with the Student's t test; the asterisk indicates $P < 0.005$, and NS indicates 'not significant difference',

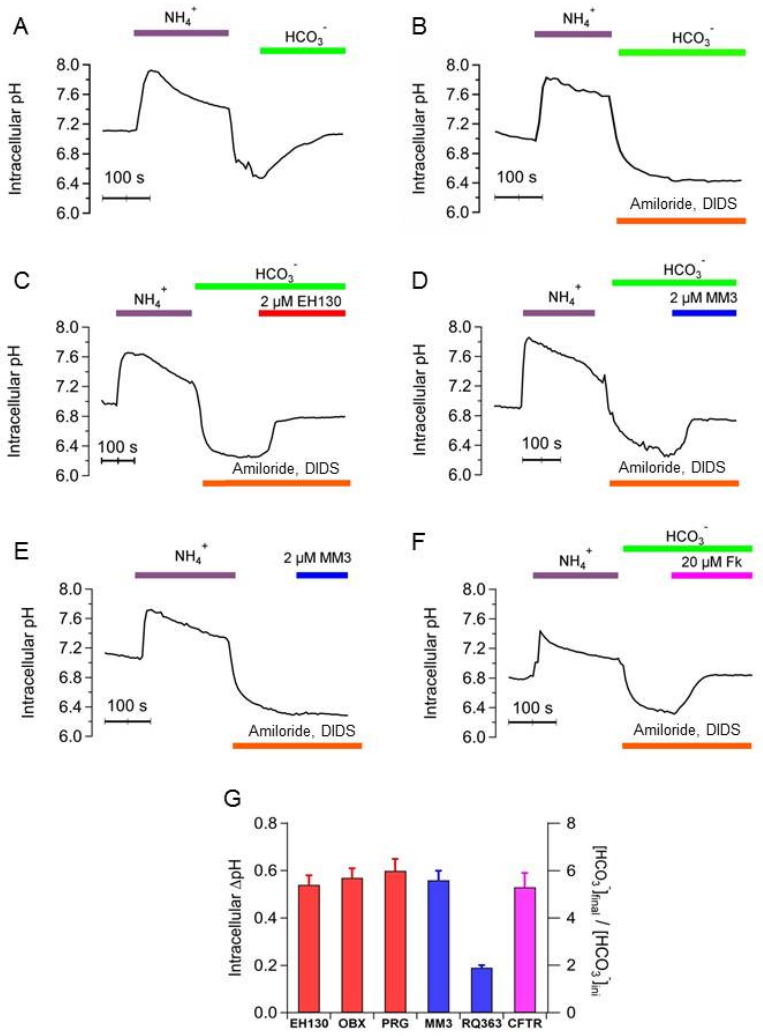


**Figure 8** Intracellular pH measured during a $NH_4^+$ pulse protocol. Perfusion of FRT (A, B, C, D) and CFTR-FRT cells (E) with solutions saturated with 5% $CO_2$ are indicated at the top of the traces. **A**: Perfusion with 40 mM $NH_4^+$ (violet bar) causes the alkalinization of the cell, followed by a fast acidification when external $NH_4^+$ is removed. Perfusion with bicarbonate (green bar) immediately induced a $pH_i$ increase, correlated with the bicarbonate influx. **B**: The main bicarbonate and proton transport mechanisms were inhibited by 1 mM amiloride and 300 µM DIDS (orange bar), and therefore there is not a $pH_i$ change. Perfusion with 2 µM EH130 (**C**, blue bar) or 2 µM MM3 (**D**, red bar), in the presence of amiloride and DIDS, induce a $pH_i$ increase correlated with bicarbonate influx. **E**: When anionophore is perfused in absence of bicarbonate there is not a $pH_i$ change. **F**: Similar experiments were performed on FRT-CFTR cells. Also in this case no $pH_i$ increase was observed until the activation of CFTR by forskolin (magenta bar). Each curve is the mean of at least 4 different regions in the acquired images. G: The change of the $pH_i$, correlated with bicarbonate influx, upon perfusion of the cells with 2 µM of the prodigiosins EH130, OBX and PRG (red bars), the tambjamines MM3 and RQ363 (blue bars), and the activation of the CFTR by 20 µM forskolin (magenta bar). Data are the mean ± SEM of 5 independent experiments.

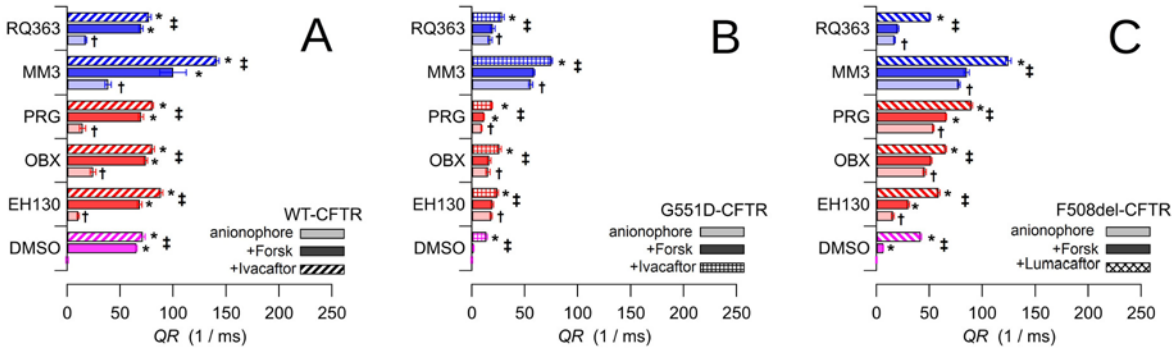


**Figure 9** Iodide influx, expressed as the initial fluorescence quenching rate, *QR*, in FRT cells expressing WT-CFTR (**A**), G551D-CFTR (**B**), and F508del-CFTR (**C**). Magenta bars indicates the control experiments with the vehicle DMSO (and not anionophore), the red bars and the blue bars are experiments with 2 µM prodigiosines and tambjamines, respectively. As shown in each panel, light colours indicate cell incubated with the sole anionophore (or the vehicle), and the strong colored bars correspond to cells treated with the anionophore plus 20 µM forskolin. WT-CFTR and G551D-CFTR cells treated with the anionophore, forskolin and 10 µM Ivacaftor are the dashed bars in **A** and **B**, respectively. F508del-CFTR cells pre-treated with 5 µM Lumacaftor overnite, and incubated with the anionophore and forskolin are the dashed bars in **C.** Bars represent the average of 5 to 12 measurements, and the SEM is indicated. The statistical significant differences ($P < 0.05$ in a Student's t test) are indicated with a dagger (†) when compares with the control with the vehicle DMSO, with an asterisk (*) when compares with the data without stimulating with foskolin, and a double dagger (‡) when compares with forskolin stimulated cels without and with Ivacaftor or Lumacaftor, respectively.